Single molecule magnet behaviour in a rare trinuclear $\{Cr^{III}Dy^{III}_2\}$ methoxo-bridged complex

Pierre-Emmanuel Car,*[a,b] Annaïck Favre,[a] Andrea Caneschi,[a] and Roberta Sessoli[a]

[a] *Dipartimento di Chimica Ugo Schiff & UdR INSTM, Università degli Studi di Firenze, Vial della Lastruccia 3-13, 50019 Sesto Fiorentino (Italy).*

[b] *Present address: Department of Chemistry, University of Zurich, Winterthurerstrasse 190, CH-8057 Zurich, Switzerland.*

Corresponding author: pierre-emmanuel.car@chem.uzh.ch

Detailed Experiment:

General Remarks

All reactions were carried out under the exclusion of moisture, unless otherwise stated. $DyCl_3 \cdot 3CH_3OH$ was synthesized following a procedure reported by Mehrotra & *al.*.[1] $CrCl_3(THF)_3$ was prepared following a procedure reported by Zeiss.[2] Sodium metal and dipivaloymethane (Hdpm) were used as received. Diethyl ether (Et_2O) was distilled from sodium/benzophenone before use. Reagent-grade methanol (CH_3OH) was carefully dried by treatment with Mg/I_2 and distilled with CaH_2 before use.[3] NaOMe was used as a 3.0 M solution in methanol freshly prepared by careful addition of sodium metal to anhydrous methanol under an inert atmosphere. Dimethoxyethane and acetonitrile were dried and distilled from CaH_2 before use.

Synthesis

$DyCl_3 \cdot 3CH_3OH$ (0.8 mmol) was dissolved in 50 mL of CH_3OH/Et_2O (v:v, 1:2). After complete dissolution, a mixture of Hdpm (1.6 mmol) in 5 mL of CH_3OH was added slowly. After 2 hours under stirring, $CrCl_3(THF)_3$ (0.267 mmol) was added and the mixture stirred until complete dissolution. To the resulting light purple solution, fresh NaOMe (3.2 mmol) was added drop by drop. The mixture was stirred 2 hours more and kept undisturbed overnight.

After one night undisturbed, the NaCl formed was removed by filtration on a G4 frit and washed two times with diethyl ether. The solution was evaporated to dryness under vacuum until getting a green residu. Then, 4 mL of fresh distilled dimethoxyethane and the tripodal ligand H_3L = 1,1,1-Tris(hydroxymethyl)-ethane (0.67 mmol) were added to the green residu, refluxed during 4 hours, cooled to room temperature and kept undisturbed overnight in a fridge.

After one night in a fridge, the mixture was filtrated and the precipitate washed with few mL of fresh distilled acetonitrile. To the filtrate, two volumes of acetonitrile were added and the mixture was refluxed 2 hours, cooled to room temperature and filtrated to evacuate residual particles. The solvent was evacuated under vacuum and the powder dissolved in diethyl ether. Single crystals suitable for X-ray diffraction analysis were obtained by vapor diffusion of methanol in a closed box. Yield: 21.8 mg, based on $DyCl_3 \cdot 3CH_3OH$ Elemental analysis calculated for $Cr_1Dy_2C_{61}O_{16}H_{115}$ (%): Cr 3.5, Dy 21.9, C 49.4, H 7.8; found: Cr 3.2, Dy 21.6, C 45.1, H 7.4.

X-ray Crystallography

A very light purple crystal of $[CrDy_2(OCH_3)_4(dpm)_5(CH_3OH)]\cdot CH_3OH$ (**1**) was mounted on a glass capillary, blocked in grease with N_2 flux (data were collected at 150 K) and transferred to a Oxford Kappa CCD diffractometer. Single crystal X-ray diffraction data were collected at 183(1) K on an *Agilent technologies XCalibur Sapphire3* area detector diffractometers equipped with single wavelength Enhance X-ray source with Mo K_α radiation (λ = 0.71069Å) from a micro-focus X-ray source. The selected suitable single crystals were mounted using polybutene oil on a flexible loop fixed on a goniometer head and immediately transferred to the diffractometer. Pre-experiment, data collection, data reduction and analytical absorption correction[4] were performed with the program suite *CrysAlisPro*.[5] Using *Olex2*,[6] the structures were solved by the *Superflip*[7] structure solution program using Charge Flipping and refined with the *SHELXL2013*[8] program package by full-matrix least-squares minimization on F^2. *Platon*[9] was used to check the results of the X-ray analyses. The *CrysAlisPro* program was used to determine the unit cell parameters and for data collection. The structure was solved by direct methods and refine against F^2 full-matrix least-squares techniques. Hydrogen atoms were included using Refxyz model (refined H-atom coordinated only). Complete crystallographic data for **1** are listed in Table S1. CCDC-1408766 for **1** contains the supplementary crystallographic data for this paper. The data can be obtained free of charge from the Cambridge Data Center (www.ccdc.cam.ac.uk/data_request/cif).

Table S1. Crystallographic data and structural refinements for compound **(1)**.

	(1)
Empirical formula	$Cr_1Dy_2O_{16}C_{61}H_{115}$
Formula weight (g.mol^{-1})	1481.54
Temperature	293 K
Radiation (λ/Å)	0.71069
Crystal system	triclinic
Space group	*P*-1
a (Å)	10.849(5)
b (Å)	14.788(5)
c (Å)	24.988(5)
α (°)	102.980(5)
β (°)	94.757(5)
γ (°)	109.062(5)
V (Å^3)	3639(2)
Z	2
ρ_{calc} (g/cm^3)	1.351
Crystal size	0.32 × 0.12 × 0.07
Reflections collected/unique	28156/11696 [R_{int} = 0.0808]
Unique observed reflections	6509
θ range (°)	4.11-24.99
F(000)	1528
Data/restraints/parameters	6509/255/783
Goodness-of-fit	0.872
R_1[a] [I>2θ(I)]	0.0518
wR_2[b]	0.1094
R_1[a] [I>2θ(I)] (all data)	0.1032
wR_2[b] (all data)	0.1196

$R_1 = \Sigma(Fo-Fc)/\Sigma Fo$ and $wR_2 = \{\Sigma w(Fo^2-Fc^2)^2/\Sigma w(Fo^2)^2\}^{1/2}$

Table S2. Selected bond distances and BVS value for **(1)**.

Bond	Distance (Å)	Bond	Distance (Å)
Cr(1)-O(1)	2.019(5)	Dy(2)-O(1)	2.449(5)
Cr(1)-O(3)	1.986(5)	Dy(2)-O(2)	2.544(5)
Cr(1)-O(4)	1.960(5)	Dy(2)-O(3)	2.478(5)
Cr(1)-O(5)	1.925(5)	Dy(2)-O(4)	2.279(5)
Cr(1)-O(14)	1.946(6)	Dy(2)-O(10)	2.293(6)
Cr(1)-O(15)	1.955(6)	Dy(2)-O(11)	2.266(6)
Dy(1)-O(1)	2.160(5)	Dy(2)-O(12)	2.336(5)
Dy(1)-O(2)	2.557(5)	Dy(2)-O(13)	2.270(6)
Dy(1)-O(3)	2.447(6)		
Dy(1)-O(5)	2.289(5)		
Dy(1)-O(6)	2.279(5)		
Dy(1)-O(7)	2.306(5)	**Atom**	**BVS value**
Dy(1)-O(8)	2.313(6)		
Dy(1)-O(9)	2.279(6)	Cr(1)	3.14

Table S3. Selected angles for **(1)**.

	Angle (°)		Angle (°)
Cr(1)-O(1)-Dy(1)	89.1(2)	Dy(1)-O(1)-Dy(2)	104.8(2)
Cr(1)-O(1)-Dy(2)	88.9(2)	Dy(1)-O(2)-Dy(2)	99.4(2)
Cr(1)-O(3)-Dy(1)	90.2(2)	Dy(1)-O(3)-Dy(2)	104.2(2)
Cr(1)-O(3)-Dy(2)	88.7(2)		
Cr(1)-O(4)-Dy(2)	95.4(2)		
Cr(1)-O(5)-Dy(1)	96.5(2)		

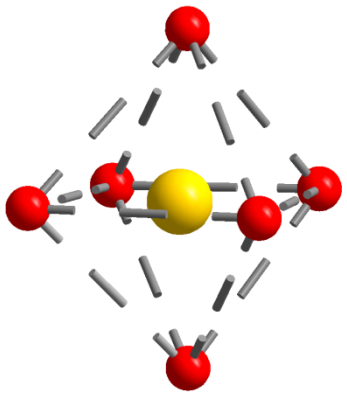

Figure S1. Representation of the octahedral geometry around Cr1. Colour code: Cr: yellow, O: red.

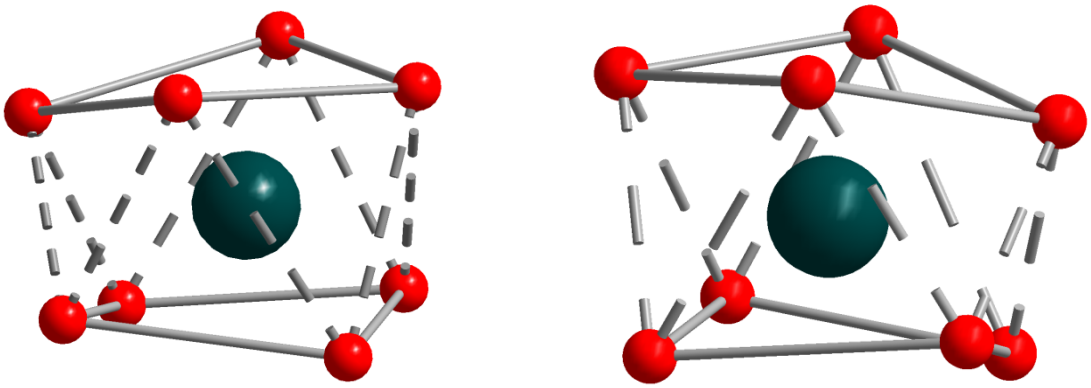

(a) **(b)**

Figure S2. Representation of the distorted square-antiprism geometry around Dy1 (left, (a)) and Dy2 (right, (b)). Colour code: Dy: teal, O: red.

Table S4. Details[10] of the structural parameters of the distorted square antiprismatic geometry of Dy1 and Dy2.

Dy1	$\Phi_{average}$	46.3°	**Dy2**	$\Phi_{average}$	46.4°
	$\alpha_{average}$	57.7°		$\alpha_{average}$	58.4°
	d_{pp}(min)	2.431(9) Å		d_{pp}(min)	2.431(9) Å
	d_{pp}(max)	3.334(1) Å		d_{pp}(min)	3.227(8) Å
	d_{in}(min)	2.637(7) Å		d_{in}(min)	2.658(9) Å
	d_{pp}(max)	3.024(8) Å		d_{in}(min)	3.090(7) Å

Φ: the skew angle between the diagonals of the two squares (45° in the ideal D_{4d} symmetry); α:the angle between the S8 axis and a Dy-O direction (magic angle of 54.74° in the ideal D_{4d} symmetry) ; d_{pp}: the distance between the two parallel O_4 squares; d_{in}: the shorter O-O distance in the O_4 square.

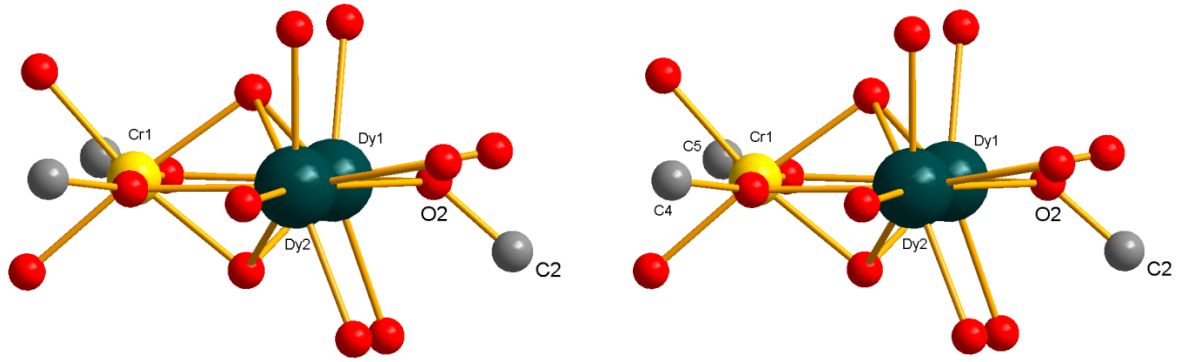

(a) **(b)**

Figure S3. Ball and stick representation of the {C2O2} arrangement out of the plan formed by {Cr1Dy1Dy2} (left, (a)); and of the arrangement of the C4 and C5 atoms.

Magnetic Investigations

Direct-current (dc) susceptibility measurements were performed by using a Quantum Design MPMS Squid magnetometer on 10.6 mg of microcrystalline $[CrDy_2(OCH_3)_4(dpm)_5(CH_3OH)].CH_3OH$ pressed in a pellet to avoid field induced orientation of the crystallites.

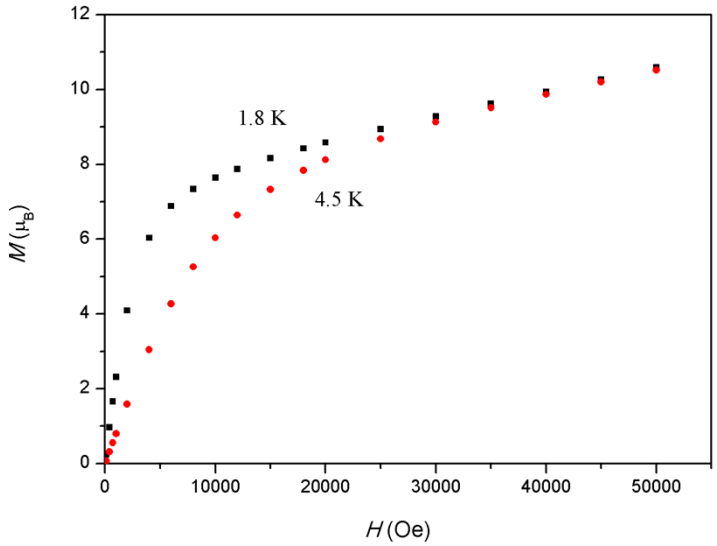

Figure S6. Field dependence of magnetization for **1**at 1.8 K and 4.5 K.

Alternating-current (ac) susceptibility measurements were performed in zero applied field on a home-made inductive probe adapted to an Oxford instruments Maglab2000 platform, between 1.6 and 6 K, under ac frequencies ranging between 0.1-60 kHz. In a second time further ac susceptibility measurements were carried out under a field 800 Oe, and ac frequencies ranging between 0.1-60 kHz.

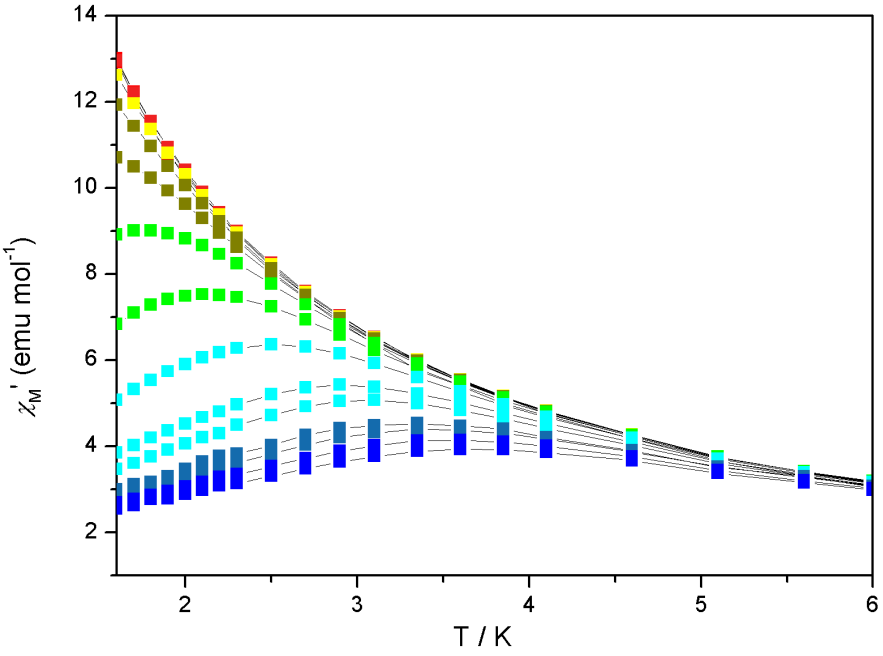

Figure S7. Temperature dependence of the in-phase χ_M', component of the molar ac susceptibility of **1** measured under zero dc field in the 1.6-6 K temperature range, and under frequencies from 0.1 (red) to 60 kHz (blue).

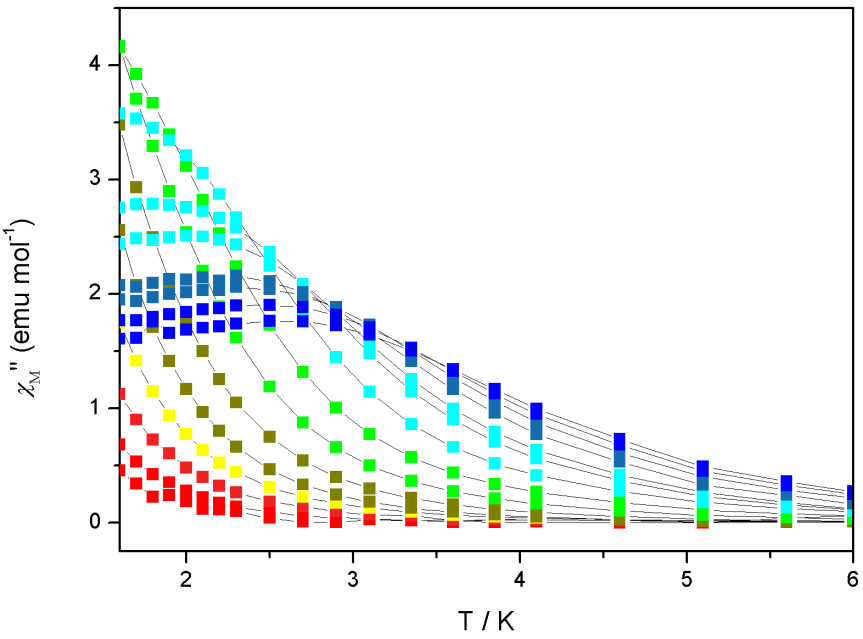

Figure S8. Temperature dependence of the out-of-phase χ_M'', component of the molar ac susceptibility of **1** measured under zero dc field in the 1.6-6 K temperature range, and under frequencies from 0.1 (red) to 60 kHz (blue).

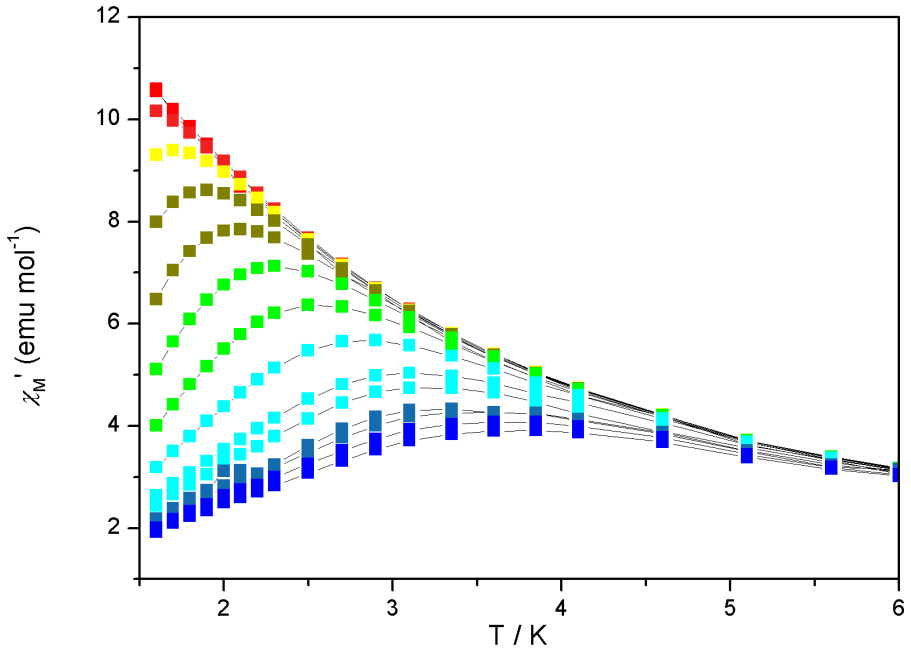

Figure S9. Temperature dependence of the in-phase χ_M', component of the molar ac susceptibility of **1** measured under a 800Oe dc field in the 1.6-6 K temperature range, and under frequencies from 0.1 (red) to 60 kHz (blue).

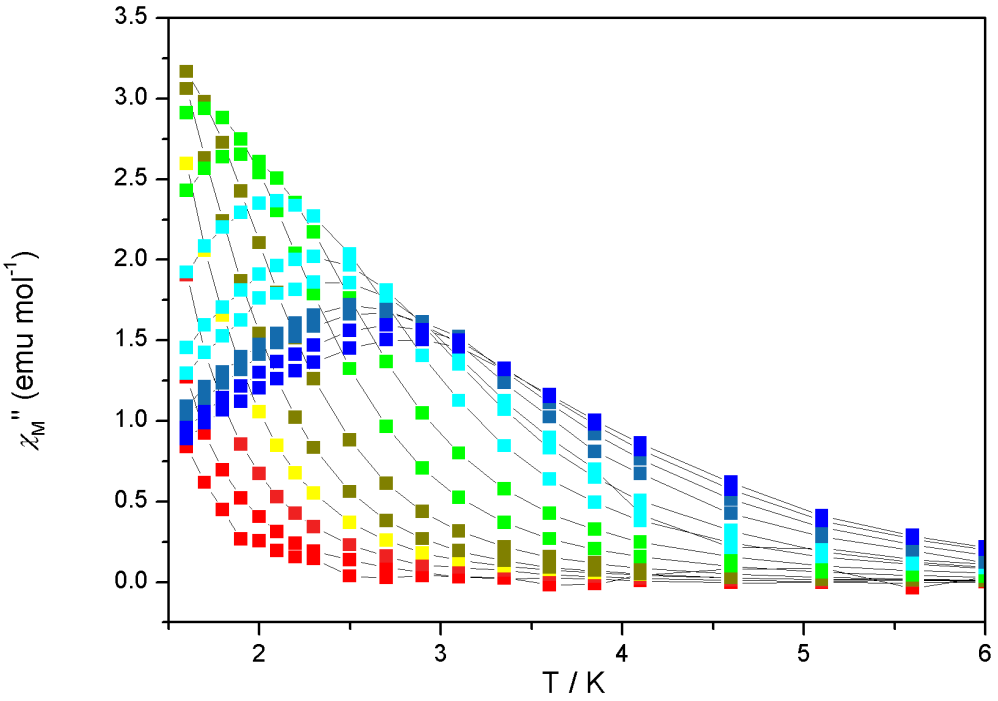

Figure S10. Temperature dependence of the out-of-phase χ_M'', component of the molar ac susceptibility of **1** measured under a 800Oe dc field in the 1.6-6 K temperature range, and under frequencies from 0.1 (red) to 60 kHz (blue).

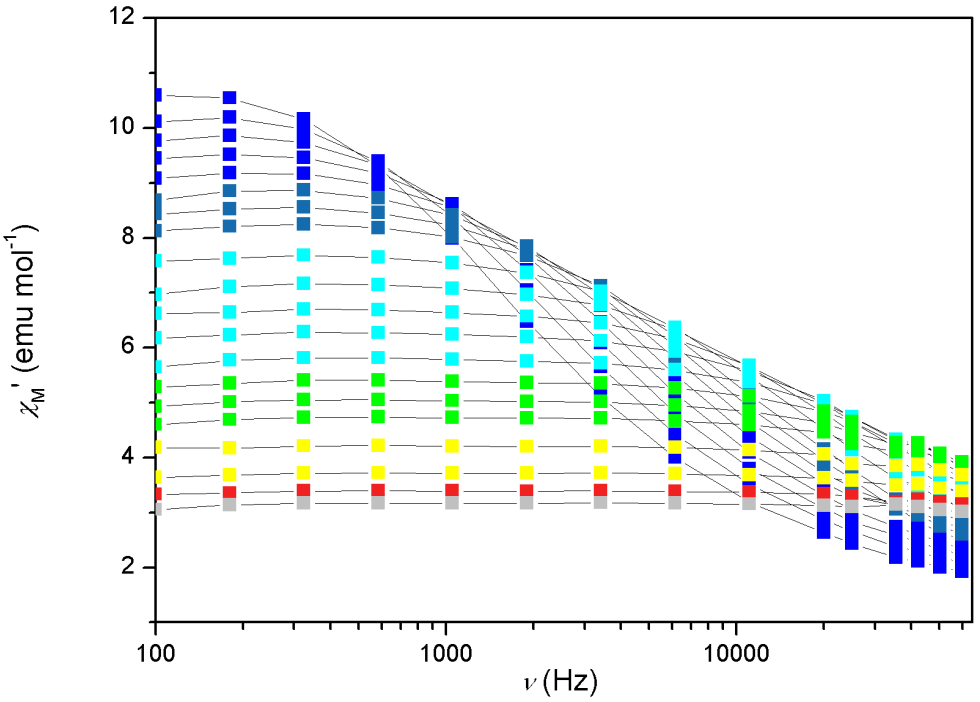

Figure S11. Frequency dependence of the in-of-phase χ_M', component of the molar ac susceptibility of **1** measured at 800Oe dc field in the 0.1-60 kHz frequency range from 1.6 (blue) to 6 K (grey).

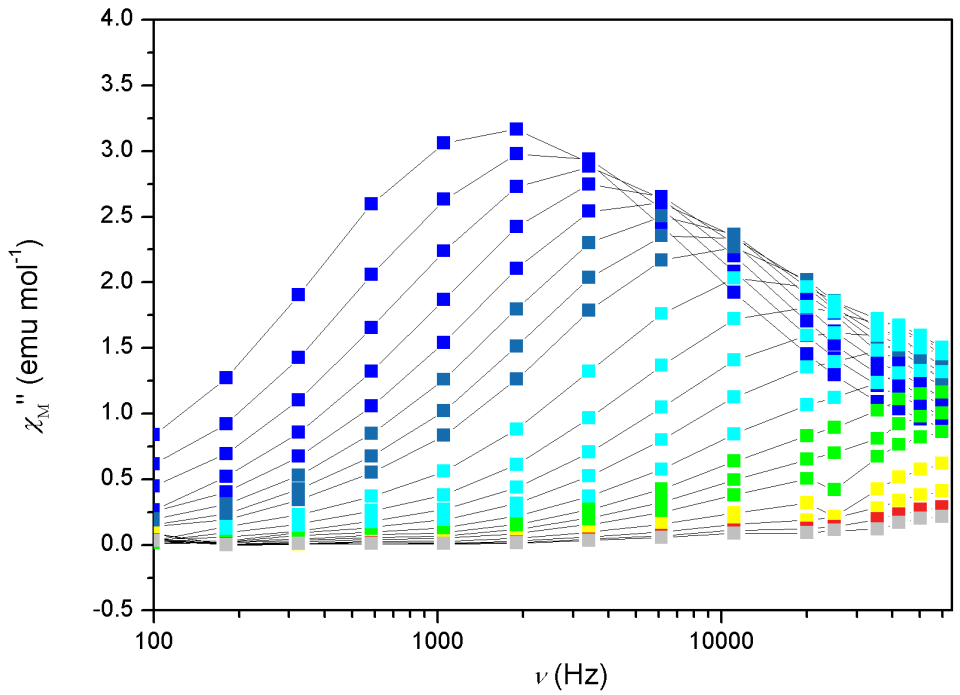

Figure S12. Frequency dependence of the out-of-phase χ_M'', component of the molar ac susceptibility of **1** measured at 800Oe dc field in the 0.1-60 kHz frequency range from 1.6 (blue) to 6 K (grey).

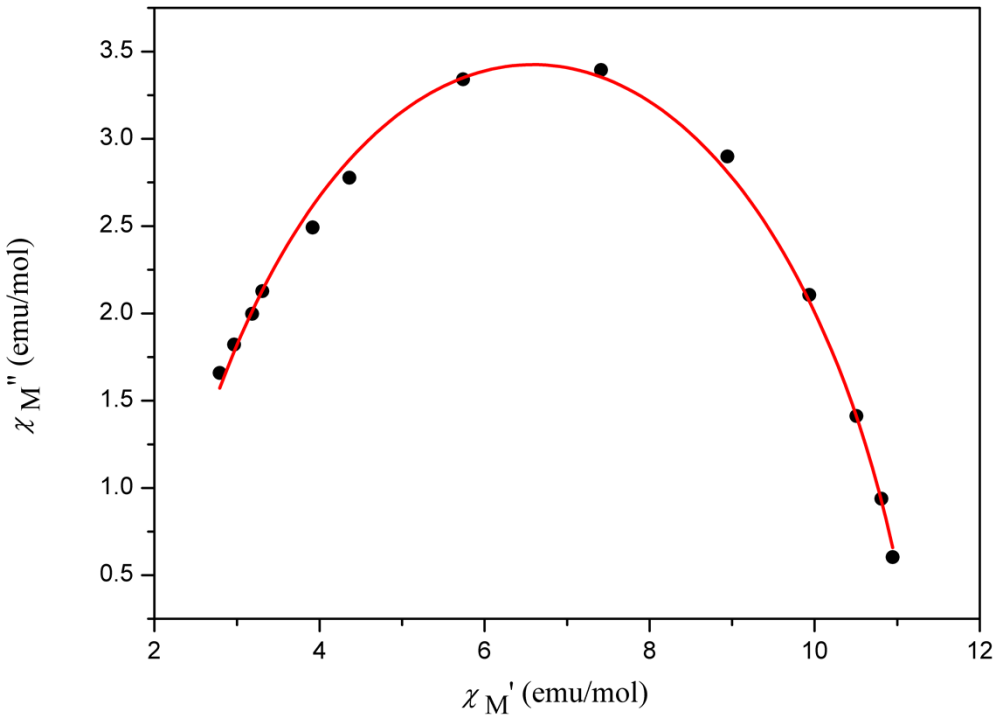

Figure S13. Example of best fit at 1.9 K (in 0 Oe dc field). Cole-Cole plot of χ_M' vs χ_M''. The red solid line represents the best fit.

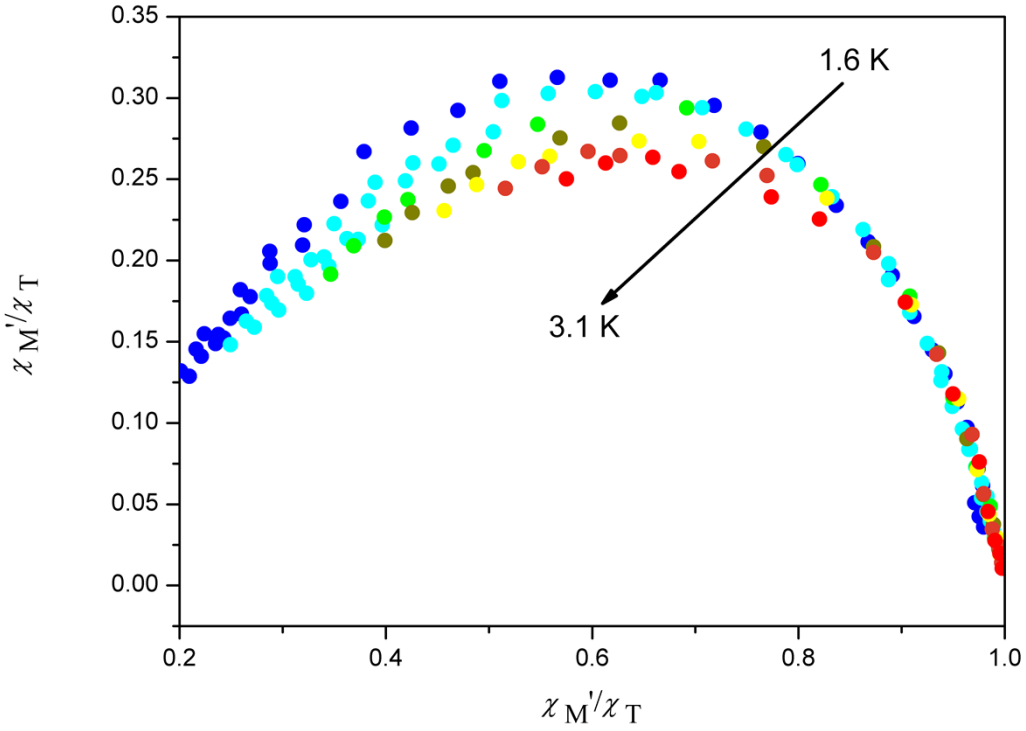

Figure S14. Argand diagram in the temperature range 1.6-3.1 K, in 0 Oe dc field. The curves were normalized by the isothermal susceptibility (χ_T). The best fits for all temperatures were omitted to facilitate the lecture.

Table S5. Main fitting parameters for the Argand plot, under a 0 Oe external field.

H(Oe)	T(K)	α	R^2	χ_T
0	1.6	0.19	0.98383	13.39
0	1.7	0.19	0.98593	12.54
0	1.8	0.18	0.98565	11.79
0	1.9	0.18	0.99323	11.19
0	2.0	0.17	0.99431	10.60
0	2.1	0.17	0.99437	10.05
0	2.2	0.16	0.99484	9.54
0	2.3	0.15	0.99586	9.08
0	2.5	0.15	0.99695	8.31
0	2.7	0.14	0.99750	7.63
0	2.9	0.14	0.99746	7.06
0	3.1	0.14	0.99766	6.56

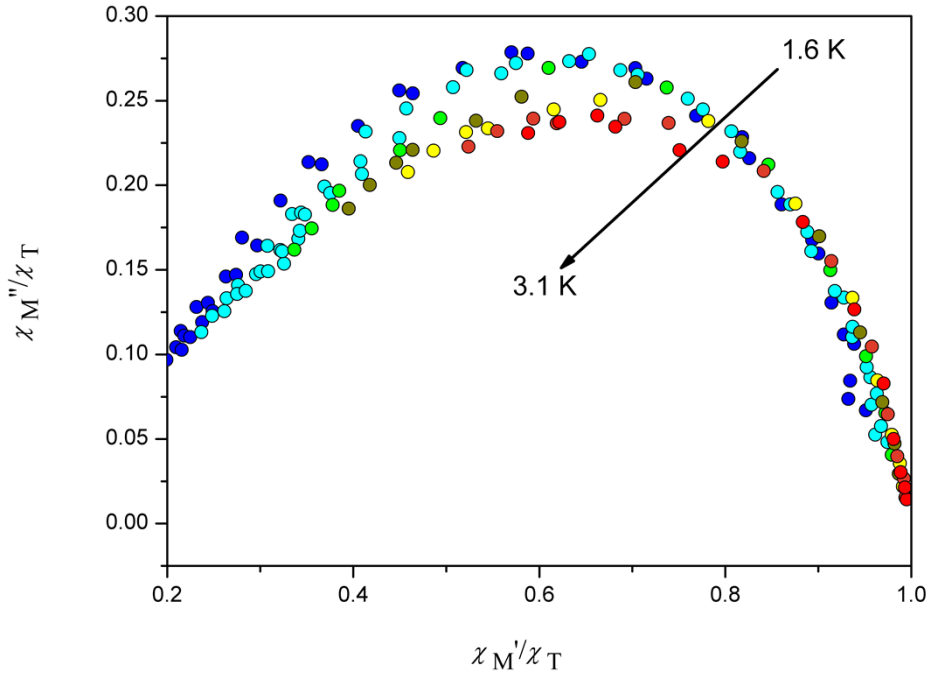

Figure S15. Argand diagram in the temperature range 1.6-3.1 K, under a 800 Oe external field. The curves were normalized by the isothermal susceptibility (χ_T). The best fits for all temperatures were omitted to facilitate the lecture.

Table S6. Main fitting parameters for the Argand plot, under a 800 Oe external field.

H(Oe)	**T(K)**	**α**	**R^2**	**χ_T**
800	1.6	0.27	0.95447	11.36
800	1.7	0.27	0.97546	10.91
800	1.8	0.26	0.97393	10.37
800	1.9	0.24	0.97031	8.89
800	2.0	0.24	0.97183	9.57
800	2.1	0.23	0.98241	9.16
800	2.2	0.22	0.98584	8.78
800	2.3	0.21	0.98784	8.42
800	2.5	0.19	0.99174	7.79
800	2.7	0.18	0.99314	7.23
800	2.9	0.17	0.99441	6.74
800	3.1	0.17	0.99438	6.31

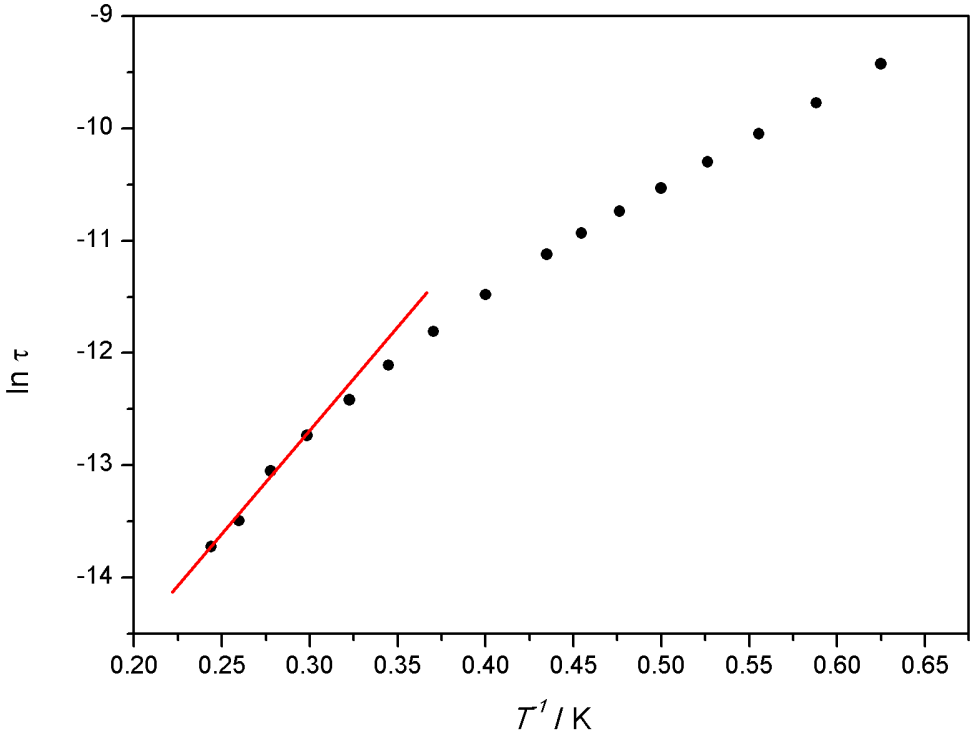

Figure S16. Arrhenius plot (under a 800 Oe external field) with best fit of the high temperature region.

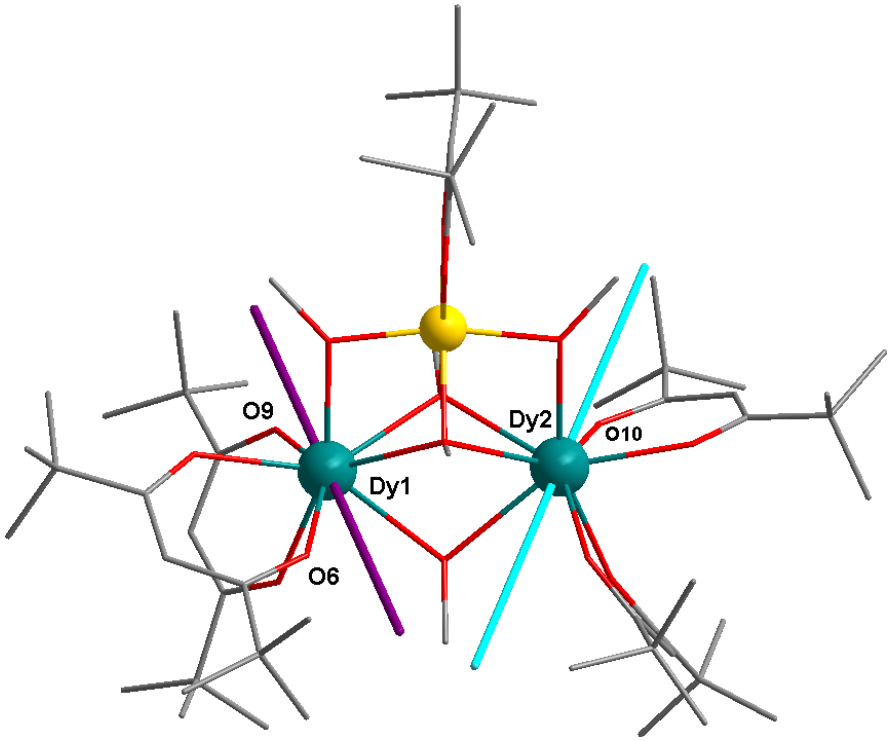

Figure S17 The ground state magnetic anisotropy directions for the Dy ions in **1**, in purple and turquoise rods for Dy1 and Dy2 ions, respectively, calculated with the electrostatic model. Dy = teal, Cr = yellow, O = red, C = grey.

References

[1] R. C. Mehrotra, T. N. Misra, S. N. Misra, *Jour. Indian Chem. Soc.*, **1965**, 42, 351.

[2] W. Herwig, H. H. Zeiss, *J. Org.Chem.*, **1958**, 23, 1404.

[3] A. I. Vogel, *Practical Organic Chemistry, Longmans: London*, **1959**, 169.

[4] R. C. Clark, J. S. Reid, *Acta Crystallographica Section A*, **1995**, 51, 887.

[5] CrysAlisPro (Oxford Diffraction Ltd.),Version 1.171.33.41, Agilent Technologies, Yarnton, Oxfordshire, England (Release 06-05-2009 CrysAlis171).

[6] O. V. Dolomanov, L. J. Bourhis, R. J. Gildea, J. A. K. Howard, H. Puschmann, *J. Appl. Cryst.*, **2009**, 42, 339.

[7] L. Palatinus, G. Chapuis, *J. Appl. Cryst.*, **2007**, 40, 786.

[8] G. Sheldrick, *Acta Crystallographica Section A*, **2008**, 64, 112.

[9] A. L. Spek, *J. Appl. Crystallogr.*, **2003**, 36, 7.

[10] (a) L. Sorace, C. Benelli, D. Gatteschi, *Chem. Soc. Rev.*, 2011, **40**, 3092; (b) G.-J. Chen, Y. Zhou, G.-X. Jin, Y.-B. Dong, *Dalton Trans.*, 2014, **43**, 16659.